

Isolation and Characterization of Current Human Coronavirus Strains in Primary Human Epithelial Cell Cultures Reveal Differences in Target Cell Tropism

Ronald Dijkman,^{a,b} Maarten F. Jebbink,^b Sylvie M. Koekkoek,^c Martin Deijis,^b Hulda R. Jónsdóttir,^a Richard Molenkamp,^c Margareta Ieven,^d Herman Goossens,^d Volker Thiel,^{a,e} Lia van der Hoek^b

Institute of Immunobiology, Kanton Hospital, St. Gallen, Switzerland^a; Laboratory of Experimental Virology, Department of Medical Microbiology, Center for Infection and Immunity Amsterdam (CINIMA), Academic Medical Center, University of Amsterdam, Netherlands^b; Laboratory of Clinical Virology, Department of Medical Microbiology, Center for Infection and Immunity Amsterdam (CINIMA), Academic Medical Center, University of Amsterdam, Netherlands^c; Department of Medical Microbiology, Vaccine and Infectious Disease Institute, University Hospital, Antwerp, Belgium^d; Vetsuisse Faculty, University of Zurich, Zurich, Switzerland^e

The human airway epithelium (HAE) represents the entry port of many human respiratory viruses, including human coronaviruses (HCoVs). Nowadays, four HCoVs, HCoV-229E, HCoV-OC43, HCoV-HKU1, and HCoV-NL63, are known to be circulating worldwide, causing upper and lower respiratory tract infections in nonhospitalized and hospitalized children. Studies of the fundamental aspects of these HCoV infections at the primary entry port, such as cell tropism, are seriously hampered by the lack of a universal culture system or suitable animal models. To expand the knowledge on fundamental virus-host interactions for all four HCoVs at the site of primary infection, we used pseudostratified HAE cell cultures to isolate and characterize representative clinical HCoV strains directly from nasopharyngeal material. Ten contemporary isolates were obtained, representing HCoV-229E ($n = 1$), HCoV-NL63 ($n = 1$), HCoV-HKU1 ($n = 4$), and HCoV-OC43 ($n = 4$). For each strain, we analyzed the replication kinetics and progeny virus release on HAE cell cultures derived from different donors. Surprisingly, by visualizing HCoV infection by confocal microscopy, we observed that HCoV-229E employs a target cell tropism for nonciliated cells, whereas HCoV-OC43, HCoV-HKU1, and HCoV-NL63 all infect ciliated cells. Collectively, the data demonstrate that HAE cell cultures, which morphologically and functionally resemble human airways *in vivo*, represent a robust universal culture system for isolating and comparing all contemporary HCoV strains.

The human airway epithelium (HAE) represents the entry port of many human respiratory viruses, including coronaviruses (CoVs). CoVs (subfamily *Coronavirinae*, family *Coronaviridae*) are positive-strand RNA viruses with the largest viral genomes of all RNA viruses (27 to 32 kb). CoV infections are associated mainly with respiratory and enteric diseases (1–3). The first reports on human CoVs (HCoVs) date back to the mid-1960s, when two human viruses, designated HCoV-229E and HCoV-OC43, were isolated from persons with the common cold (4, 5). HCoVs are associated with mild respiratory tract disease (common cold) that may cause more severe symptoms in elderly or immunocompromised individuals (6–11). However, the appearance of severe acute respiratory syndrome (SARS), caused by a formerly unknown coronavirus, SARS-CoV, and the most recent identification of another human coronavirus, HCoV-EMC, exemplify the considerable zoonotic potential of coronaviruses and their ability to seriously affect human health (2, 12–17). In the aftermath of the SARS pandemic, the number of newly identified CoVs and host species is continuously increasing (2, 18–20). Intensified global virus discovery efforts have also revealed that more HCoVs exist, as demonstrated by the identification of HCoV-NL63 in 2004 and HCoV-HKU1 in 2005 (19, 20). Both viruses are not emerging viruses, like SARS-CoV and HCoV-EMC, but were previously unidentified. Infections by these viruses are as common and widespread as HCoV-229E and HCoV-OC43 infections (11, 21).

Despite the accumulating knowledge on HCoV prevalences and disease burdens, studies on fundamental aspects of HCoV infections regarding target cell tropism and other crucial virus-host interactions are seriously hampered by the lack of a universal

cell culture system or suitable animal models that allow propagation of all four currently known HCoVs. The fastidious nature of HCoVs on conventional cell lines was described during the mid-1960s and led to *ex vivo* culturing of human embryo respiratory tract explants (4, 5, 22, 23). Currently, the pseudostratified HAE cell culture system is used as an alternative and convenient *in vitro* tool to propagate and characterize newly identified human respiratory viruses (24). Thus far, one isolate of HCoV-HKU1—which is refractory to propagation on conventional cell lines—has been cultured on HAE (25), as well as the reference strain of HCoV-NL63 (26).

In this study, we used HAE cell cultures as a universal cell culture system to isolate and characterize all four contemporary HCoV strains. In total, we obtained 10 contemporary clinical isolates among 18 HCoV-positive nasopharyngeal specimens, encompassing four HCoV strains: HCoV-229E ($n = 1$), HCoV-NL63 ($n = 1$), HCoV-HKU1 ($n = 4$), and HCoV-OC43 ($n = 4$). For each strain, we used one isolate to analyze the replication kinetics and progeny virus release on HAE cell cultures established from primary cells from different donors. Furthermore, by using confocal microscopy, we determined the target cell tropism of

Received 6 December 2012 Accepted 25 January 2013

Published ahead of print 20 February 2013

Address correspondence to Lia van der Hoek, c.m.vanderhoek@amc.uva.nl.

Copyright © 2013, American Society for Microbiology. All Rights Reserved.

doi:10.1128/JVI.03368-12

each HCoV strain by visualizing intracellular double-stranded RNA (dsRNA) and/or viral proteins in human airway epithelia.

MATERIALS AND METHODS

Virus stocks. The HCoV-NL63 (isolate Amsterdam 1 [Ams-001]) virus stock was obtained by inoculating a monolayer of LLC-MK2 cells as described previously (19). The supernatant was harvested after 7 days and stored in aliquots at -80°C , after removal of cellular debris by centrifugation. HCoV-229E (Inf-1) cell culture supernatant was obtained as previously described (27). HCoV-OC43 (VR-759) was obtained from the ATCC.

Clinical material. Twelve nasopharyngeal specimens were collected in January 2010 at the Laboratory of Clinical Virology, Department of Medical Microbiology, Academic Medical Center, Amsterdam, Netherlands, from patients who were hospitalized due to upper or lower respiratory tract illness. Research on the samples was conducted in accordance with the ethical principles set out in the Declaration of Helsinki. Viral infections were determined with an in-house diagnostic quantitative reverse transcription-PCR (qRT-PCR) panel for human respiratory viruses. All nasopharyngeal washes used in this study were positive for HCoVs and negative for human bocavirus, human metapneumovirus, influenza A and B viruses, respiratory syncytial virus, human picornaviruses, human adenovirus, and human parainfluenza viruses 1 to 4 (28). One HCoV-NL63 clinical sample has been described previously (29). Five additional HCoV-NL63-positive nasopharyngeal specimens that were negative for human bocavirus, human metapneumovirus, influenza A and B viruses, respiratory syncytial virus, human picornaviruses, human adenovirus, and human parainfluenza viruses 1 to 4 were obtained from the EU-financed GRACE study (<http://www.grace-lrti.org>). The following ethics review committees approved the study: in Cardiff and Southampton, United Kingdom, Southampton & South West Hampshire Research Ethics Committee A; in Utrecht, Netherlands, Medisch Ethische Toetsingscommissie Universitair Medisch Centrum Utrecht; in Barcelona, Spain, Comitè Ètic d'Investigació Clínica Hospital Clínic de Barcelona; in Mataro, Spain, Comitè d'Ètica d'Investigació Clínica (CEIC) del Consorci Sanitari del Maresme; in Rothenburg, Germany, Ethik-Kommission der Medizinischen Fakultät der Georg-August-Universität Göttingen; in Antwerp, Belgium, UZ Antwerpen Comité voor Medische Ethiek; in Lodz, Szczecin, and Białystok, Poland, Komisja Bioetyki Uniwersytetu Medycznego W Lodzi; in Milan, Italy, IRCCS Fondazione cà Granda Policlinico; in Jonkoping, Sweden, Regionala Etikprövningsnämnden i Linköping; in Bratislava, Slovakia, Etika Komisia Bratislavského; in Gent, Belgium, Ethisch Comité Universitair Ziekenhuis Gent; in Nice, France, Comité de Protection des Personnes Sud-Méditerranée II, Hôpital Salva-tor; and in Jesenice, Slovenia, Komisija Republike Slovenije za Medicinsko Etiko. Written informed consent was provided by all study participants.

Human airway epithelial cell culture. Normal primary human bronchial epithelial cells (HBEpC) were isolated from patients (>18 years old) who underwent bronchoscopy and/or surgical lung resection in their diagnostic pathway for any pulmonary disease and who gave informed consent. This was done in accordance with local regulations from the Academic Medical Center, Netherlands, or the Kantonal Hospital St. Gallen, Switzerland, as part of the St. Gallen Lung Biopsy Biobank (SGLBB), which received approval by the ethics committee of the Canton St. Gallen (EKSG 11/044, 27 April 2011). Pathologically examined bronchial segments were incubated for 48 h at $+4^{\circ}\text{C}$ in minimal essential medium (MEM; Sigma) supplemented with a mixture of protease XIV-DNase I (Sigma) and the following additives (Sigma): penicillin G sulfate (100 units/ml), streptomycin sulfate (100 $\mu\text{g}/\text{ml}$), amphotericin B (1.25 $\mu\text{g}/\text{ml}$), gentamicin (50 $\mu\text{g}/\text{ml}$), and nystatin (100 units/ml). After cell dissociation, the HBEpC were maintained for one or two serial passages as a monolayer in bronchial epithelial cell serum-free growth medium (BEGM) (30), which is LHC basal medium (Invitrogen) supplemented with the required additives (Sigma and Sciencecell). BEGM was refreshed at 2- or 3-day intervals. Subpassaging of HBEpC to form pseudostratified

human airway epithelial cell cultures was done as described previously (24). The washing of the apical surface was adjusted to 7-day intervals. Prior to the experiments, all cultures were maintained at 37°C in a 5% CO_2 incubator.

Human coronavirus infection. An aliquot of 50 μl of clinical patient material or cell culture supernatant was diluted in 200 μl Hanks balanced salt solution (HBSS) and centrifuged for 4 min at room temperature at a $1,500\times$ relative centrifugal force (RCF). Two hundred microliters of diluted clinical sample was directly inoculated onto the apical surface of pseudostratified human airway epithelium and incubated for 2 h at 33°C in a 5% CO_2 incubator. After 2 h, the inoculum was collected and stored in an equal volume of homemade virus transport medium (VTM; MEM supplemented with 0.5% gelatin). The apical surface was rinsed three times with 500 μl of HBSS, and inoculated cultures were maintained at 33°C in a 5% CO_2 incubator. Samples were collected from the apical surface or the basolateral compartment at the indicated time points post-inoculation. Apical harvesting was performed by adding 200 μl of HBSS to the apical surface, incubating the culture for 10 min at 33°C in a 5% CO_2 incubator, and then removing and storing the apical surface in an equal volume of VTM. From the basolateral compartment, 200 μl of medium was transferred into an equal volume of VTM, after which an equal volume of fresh medium was supplemented with the remaining medium in the basolateral compartment. Cultures were observed daily by eye, using a phase-contrast microscope.

RNA isolation and cDNA synthesis. Viral RNA was isolated from 100 μl of apical or basolateral harvest by using the Boom method for total nucleic acid isolation (31); elution was performed in 100 μl RNase-free H_2O . Alternatively, viral RNA was isolated from the collected samples by use of a NucleoSpin RNA II kit according to the manufacturer's protocol (Macherey-Nagel); elution was performed in 60 μl RNase-free H_2O . Reverse transcription was performed with Moloney murine leukemia virus reverse transcriptase (Invitrogen) (200 units) and 12.5 ng of random primers (Invitrogen) in a solution containing 10 mM Tris, pH 8.3, 50 mM KCl, 0.1% Triton X-100, 6 mM MgCl_2 , and a 25 μM concentration of each deoxynucleoside triphosphate, in a total volume of 20 μl , at 37°C for 60 min.

Human coronavirus kinetics. Genotyping and quantification of viral HCoV RNA yields were performed using a Platinum quantitative PCR SuperMix–uracil-DNA glycosylase (UDG) kit (Invitrogen). Ten microliters of cDNA was amplified in 50 μl $1\times$ Platinum quantitative PCR SuperMix–uracil-DNA glycosylase (Invitrogen) with 5.0 mM MgCl_2 , 10 μM specific probe labeled with 6-carboxyfluorescein (FAM) and 6-carboxy-tetramethylrhodamine (TAMRA), and 45 μM (each) primers. Primers targeting HCoV-NL63, HCoV-HKU1, HCoV-229E, and HCoV-OC43 are described elsewhere (25, 32, 33). Measurements were done with an ABI Prism 7000 sequence detection system (Applied Biosystems, Foster City, CA). Following the UDG treatment for 2 min at 50°C and denaturing for 10 min at 95°C , 45 cycles of amplification (15 s at 95°C and 60 s at 60°C) were performed.

Quantification of viral HCoV RNA yields of contemporary strains was performed using LightCycler 480 Probes master mix (Roche). Two microliters of cDNA was amplified according to the manufacturer's protocol, using the above-mentioned sense and antisense strain-specific primers. Measurements and analysis were performed on a LightCycler 480 II instrument, using the LightCycler 480 software package (Roche). The cycle profile was 10 min at 95°C followed by 45 cycles of 10 s at 95°C , 20 s at 60°C , and 30 s at 72°C and then a melting curve step to confirm product specificity.

Confocal microscopy analysis. Infected HAE cultures were fixed with 4% paraformaldehyde (PFA; FormaFix) for 30 min at room temperature, followed by rinsing of the apical and basolateral sides three times with 1 ml of phosphate-buffered saline (PBS). Fixed HAE cultures were immunostained using a previously described procedure (34). For simultaneous detection of HCoV proteins and ciliated cells, human intravenous immunoglobulin (IVIg) (1:500; 50 mg/ml) (Nanogam, Sanquin B.V.) and

mouse monoclonal anti- β -tubulin IV (1:400) (Sigma) were applied as primary antibodies. Donkey-derived Dylight 488-labeled anti-mouse IgG(H+L) and Dylight 594-labeled anti-human IgG(H+L) (1:200) (Jackson ImmunoResearch) were applied as secondary antibodies. For detection of dsRNA, viral replication complexes, tight junctions, and ciliated cells, monoclonal anti-dsRNA (J2; English & Scientific Consulting Bt.), anti-HCoV-229E NSP8 (1:400; kindly provided by John Ziebuhr [35]), and goat polyclonal anti-ZO1 (1:200; Abcam) were applied as primary antibodies. Donkey-derived Dylight 488-labeled anti-mouse IgG(H+L), Dylight 549-labeled anti-goat IgG(H+L), and Dylight 647-labeled anti-rabbit IgG(H+L) (Jackson ImmunoResearch) were applied as secondary antibodies, followed by a separate incubation with Cy3-conjugated mouse anti- β -tubulin (1:1,000; Sigma) for staining of ciliated cells. The above-described staining combinations were all counterstained with DAPI (4',6-diamidino-2-phenylindole; Invitrogen) before the membranes were dissected and mounted under a coverslip on a glass slide with Vectashield mounting medium (Vector Laboratories). Fluorescence images were acquired using an EC Plan-Neofluor 40 \times /1.30 oil differential interference contrast (DIC) M27 or Plan-Apochromat 63 \times /1.40 oil DIC M27 objective on a Zeiss LSM 710 confocal microscope. Image capture, analysis, and processing were performed using the ZEN 2010 (Zeiss) and Imaris (Bitplane Scientific Software) software packages.

Cryosections. For *in vivo* and *in vitro* examinations of the CD13 distribution in the human airway epithelium, primary bronchial segments and pseudostratified HAE cell cultures were fixed with 4% PFA (Forma-Fix) for 30 min at room temperature, followed by rinsing of the samples three times with PBS. Fixed samples were mounted in Tissue-Tek OCT medium and snap-frozen in liquid nitrogen, and then 10- μ m-thick horizontal sections were made. Monoclonal anti- β -tubulin (Sigma) and sheep polyclonal anti-human CD13 (R&D Systems) were applied as primary antibodies. Donkey-derived Dylight 488-labeled anti-mouse IgG(H+L) and Cy3-labeled anti-sheep IgG(H+L) (Jackson ImmunoResearch) were applied as secondary antibodies and were counterstained with DAPI (Invitrogen), using the procedure described above.

Statistical analysis. Calculations were performed using Prism software, version 5 (Graphpad). Comparison of the colocalization percentages of dsRNA with nonciliated and ciliated cells for four contemporary HCoV strains at 96 h postinoculation (hpi) was performed using a two-tailed, unpaired *t* test with a threshold for significance of a *P* value of <0.05.

RESULTS

Isolation of clinical HCoV strains by use of HAE cultures. The currently available laboratory-adapted reference strains of HCoV-229E and HCoV-OC43 are known to differ from clinical strains with respect to deletions or mutations in the structural and accessory genes (36, 37). We therefore aimed to isolate representative clinical HCoV strains directly from nasopharyngeal aspirate (NPA) specimens. We initially used an unbiased approach and assessed 12 NPA specimens that were found to be HCoV positive by a pan-HCoV qPCR and were negative for human bocavirus, human metapneumovirus, influenza A and B viruses, respiratory syncytial virus, human picornaviruses, human adenovirus, and human parainfluenza viruses. An aliquot of 50 μ l of each sample was diluted 1:5 in HBSS, and then 200 μ l of diluted sample was used to inoculate the apical surface of a pseudostratified HAE cell culture. The inoculants were incubated for 2 h at 33°C, followed by removal and rinsing of the apical surface three times with HBSS to remove any residual unbound viral particles. During the infection, the cultures were maintained at 33°C, and 200- μ l harvests were collected from the apical surface at 2, 24, 48, 72, 96, 120, 144, and 168 hpi. Quantification of the viral yields within the sequential samples taken from the 12 HCoV cultures showed a steep

increase of viral RNA yields for 9 of the 12 HAE cell cultures around 48 hpi, which increased and reached a plateau between 72 and 120 hpi (Fig. 1A to C). By subsequent determination of the genotype of each clinical isolate by strain-specific real-time PCRs, we assigned four isolates to HCoV-HKU1, one isolate to HCoV-229E, and four isolates to HCoV-OC43 (Fig. 1A to C). As shown in Table 1, the clinical isolates that could be isolated directly from diluted NPA specimens and propagated upon the HAE cell cultures had viral RNA concentrations in the range of 157 to 153×10^5 genome copies per milliliter. When we determined the HCoV genotypes of the three NPA samples that did not yield detectable virus replication following inoculation of HAE cultures, we noticed that they did not contain any HCoV-NL63-specific sequences. Therefore, six additional clinical specimens known to be positive for HCoV-NL63 were selected to isolate new contemporary HCoV-NL63 isolates. Inoculation of HAE cultures with these HCoV-NL63-positive specimens revealed that a steep increase of viral RNA yields could be detected for only one isolate (R2354) (Fig. 1D). Determining the HCoV-NL63 RNA concentration demonstrated that it ranged from 5.49×10^3 to 1.49×10^7 genome copies per milliliter (Table 1). Repetition of the experiment by use of HAE cultures from a different donor did not improve the recovery rate (data not shown). Therefore, the low isolation rate of new HCoV-NL63 isolates directly from clinical specimens (isolation from only one of six specimens) suggests that HCoV-NL63 is more difficult to isolate than the other three HCoV species (Table 1). Collectively, these data demonstrate that the HAE culture system is suitable for isolation and propagation of all four contemporary HCoV strains.

Progeny virus release. The successful propagation of clinical isolates of each of the four circulating HCoV strains gave us the opportunity to analyze their replication kinetics and progeny virus release characteristics within a single cell culture system. We first compared virus replication of the clinical HCoV-OC43, HCoV-NL63, and HCoV-229E isolates to that of their respective laboratory-adapted reference strains. Inoculation of HAE cultures was done as described above, using approximately 5×10^5 genome copies per milliliter. The release of progeny virus at the apical surface was monitored at 24, 48, 72, and 96 hpi. No gross differences concerning the replication kinetics were observed between the clinical isolates and the laboratory reference strains of HCoV-OC43 and HCoV-229E (Fig. 2A and B). For HCoV-NL63, the reference strain reached higher titers than those of the clinical isolate (Fig. 2C). These initial results indicated that the genomic alterations in the HCoV-OC43 and HCoV-229E reference strains did not seem to influence their replication kinetics in the human airway epithelium.

We addressed the robustness of the HAE cell culture system by using primary epithelial cells from different donors. A single representative isolate of each HCoV strain was chosen from the pool of newly isolated contemporary HCOVs, except for HCoV-NL63. Because of the low replication kinetics of and limited amount of NPA material containing the HCoV-NL63 clinical strain (R2354), we decided to use the HCoV-NL63 reference strain (Ams-001) instead. Indeed, the HCoV-NL63 reference strain was isolated in 2004, its genome sequence is >99% identical to those of clinical isolates (29), and it has a well-documented passage history of no more than 8 passages in standard cell culture (LLC-MK2 cells). Therefore, it can be considered a contemporary clinical isolate. The inoculum to infect HAE cultures was standardized to 1×10^5

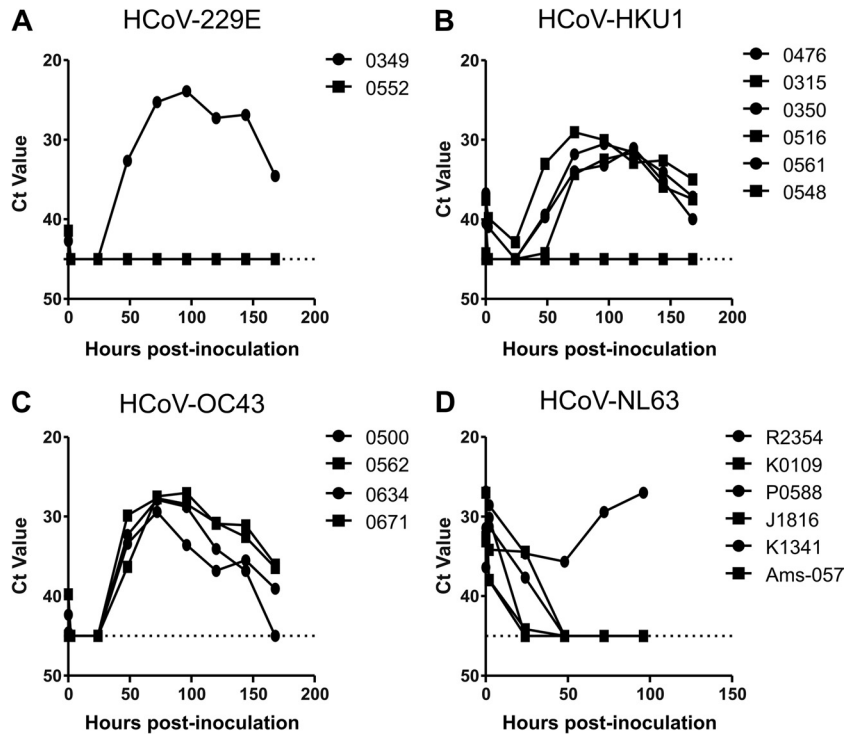


FIG 1 Isolation of clinical HCoV isolates on HAE cell cultures infected with HCoV-positive nasopharyngeal aspirates, from which the viral yield was monitored. Viral yields are given as C_T values (y axis) at the indicated times postinoculation (x axis) for clinical HCoV-229E (A), HCoV-HKU1 (B), HCoV-OC43 (C), and HCoV-NL63 (D) isolates. The horizontal dashed line represents the detection threshold of the HCoV real-time PCR. The results of a representative experiment are shown.

genome copies per 200 μ l. Replication kinetics of the HCoV-NL63 (Ams-001), HCoV-229E (0349), HCoV-HKU1 (0315), and HCoV-OC43 (0500) strains were determined on HAE cultures derived from three different donors. The same experimental conditions as those described above were used, except that the release

of progeny viral RNA was monitored at 2, 24, 48, 72, 96, and 120 hpi for the apical surface and at 48 and 120 hpi for the basolateral compartment. We observed that the replication kinetics at the apical surface for HCoV-229E and HCoV-HKU1 were comparable, with a 2- to 3-log increase in the viral RNA yield within the first 72 hpi (Fig. 3). However, in cells from one donor (3011), we observed reduced viral growth kinetics for both viruses during the first 72 h, but eventually the viral RNA yields were similar to those observed for the other two donors at 120 hpi (Fig. 3). Visual observation of the cultures revealed no gross morphological differences among the different HAE cultures; thus, this lag period was likely influenced by an as yet undefined mechanism. This effect was not observed for HCoV-NL63 and HCoV-OC43, which showed robust kinetics among the different donors (Fig. 3). In the basolateral compartment, we detected incidental oscillation of the viral RNA among the basolateral medium samples for each of the HCoV species. However, in all cases, the viral RNA concentration was several orders of magnitude lower (≥ 3 log) than the apical secreted RNA yield (Fig. 3E). These results demonstrate that the HAE cell culture system is robust and reveal a predominant apical polarity of progeny virus release for all four HCoVs.

Cell tropism. HCoV-NL63 and HCoV-HKU1 are known to employ a target cell tropism predominantly for ciliated cells on HAEs. However, similar studies to determine the target cell tropism of HCoV-229E and HCoV-OC43 have not yet been reported. Therefore, we examined HCoV-229E- and HCoV-OC43-infected HAE cultures at 96 hpi, in parallel with infections by HCoV-NL63 and HCoV-HKU1. The infections were performed with contemporary HCoV-229E (0349), HCoV-OC43 (0500),

TABLE 1 Isolation of representative clinical HCoV strains

Strain	Isolate	Viral load (genome copies/ml)	Replication
HCoV-229E	552	6.67E+03	No
	349	6.58E+03	Yes
HCoV-NL63	R2354	1.53E+07	Yes
	P0588	5.89E+05	No
	J1816	5.01E+04	No
	K1341	9.14E+03	No
	K0109	5.49E+03	No
	Ams-057	1.09E+06	No
HCoV-HKU1	516	4.71E+06	Yes
	561	7.11E+05	No
	476	1.33E+05	Yes
	315	1.46E+04	Yes
	548	6.88E+02	No
	350	2.77E+03	Yes
HCoV-OC43	500	1.57E+02	Yes
	671	3.43E+03	Yes
	634	1.66E+02	Yes
	562	3.28E+03	Yes

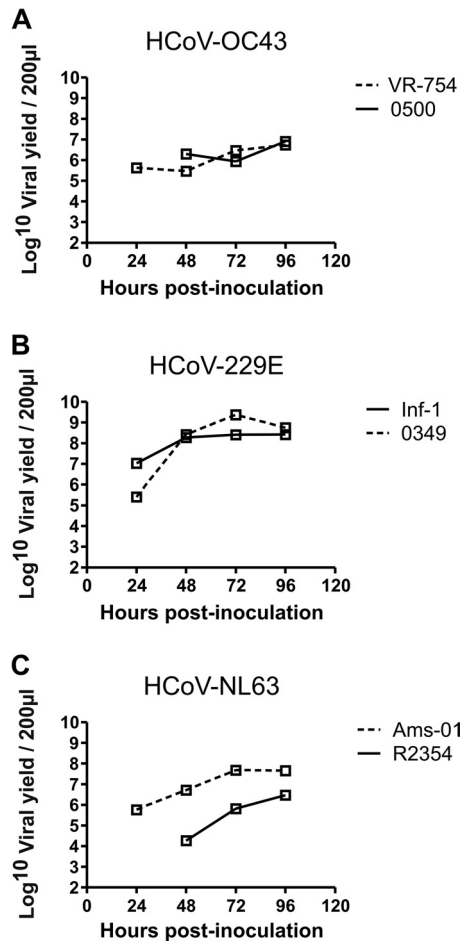


FIG 2 Viral yields of cell culture reference strains versus representative clinical isolates. The monitored viral yields (genome copies/200 µl; y axis) at the indicated times postinoculation (x axis) are given for the cell culture-adapted reference strains and representative clinical isolates of HCoV-OC43 (A), HCoV-229E (B), and HCoV-NL63 (C). The results of a representative experiment are shown.

HCoV-HKU1 (0315), and HCoV-NL63 (R2354) isolates and with the reference strains of HCoV-OC43 (VR759), HCoV-229E (Inf-1), and HCoV-NL63 (Ams-001). No changes in cell layer confluence, morphology, or cilium movement were observed in any of the HCoV-inoculated cultures compared with the control culture. We used human IVIg to detect viral proteins in infected cells, and a β-tubulin antibody was applied to discriminate between ciliated and nonciliated cell populations. As shown in Fig. 4, confocal microscopy revealed that IVIg could be used to detect viral antigens in HAE cultures for all four clinical HCoV isolates (Fig. 4). The colocalization results show that IVIg-positive cells in HCoV-OC43-, HCoV-HKU1-, and HCoV-NL63-infected HAE cultures were predominantly ciliated cells. In contrast, and surprisingly, HCoV-229E-infected cells were predominantly nonciliated (Fig. 4). The same results were obtained by infecting HAE cultures with the corresponding laboratory reference HCoV strains (data not shown).

The usage of IVIg in immunofluorescence detection of HCoV-infected cells in HAE cultures is limited to only those HCoV strains that are continuously circulating in the human population.

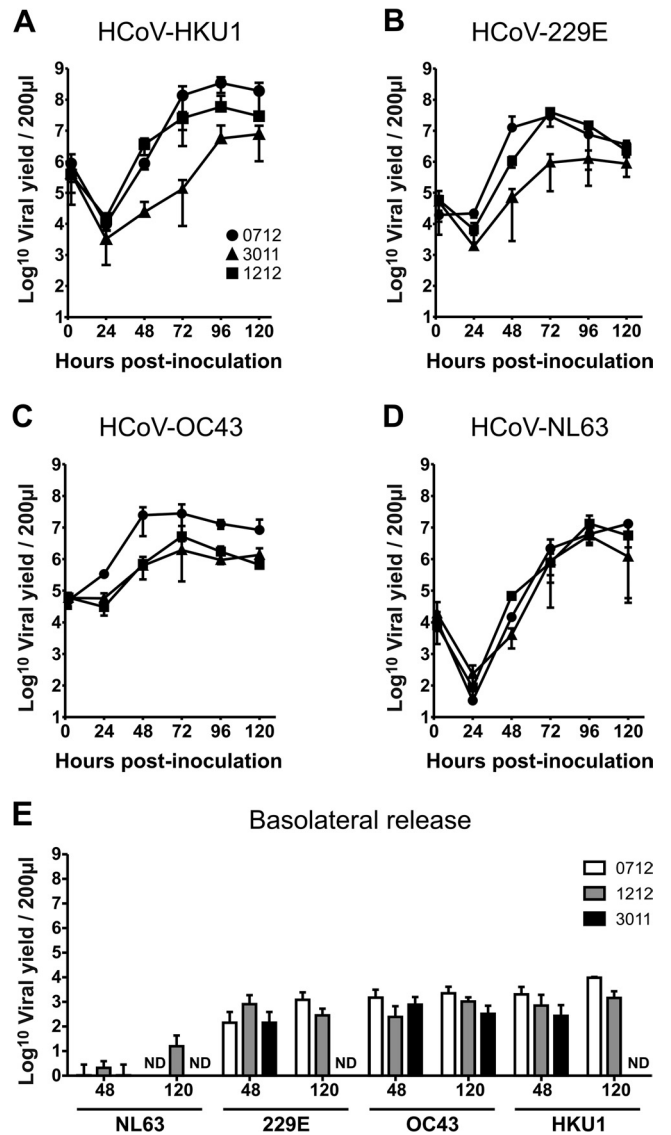


FIG 3 Characteristics of contemporary HCoV strains on HAE from different donors. The monitored apical viral yields are given as viral RNA yields per 200 µl at the indicated times postinoculation for contemporary HCoV-HKU1 (A), HCoV-229E (B), HCoV-OC43 (C), and HCoV-NL63 (D) strains. (E) The monitored basolateral viral yields at 48 and 120 hpi are given for the indicated contemporary HCoV strains. The results are shown as means and standard deviations (SD) for triplicates from 3 independent experiments. ND, not detected.

Furthermore, the antibody concentration within the human serum pool can differ concerning specificity for particular HCoV strains, but also concerning the level of viral antigen expression that can reproducibly be detected. Therefore, we employed an antibody directed against dsRNA as an alternative to eliminate these variables. This monoclonal antibody has been shown to bind dsRNA independent of sequence and nucleotide composition (38) and can thus detect each HCoV strain and species, independent of their genomic composition. To evaluate the antibody in our setting, we used HCoV-229E (Inf-1)- and mock-infected HAE cultures together with an antibody against the HCoV nonstructural protein 8 to confirm the specificity of the dsRNA antibody.

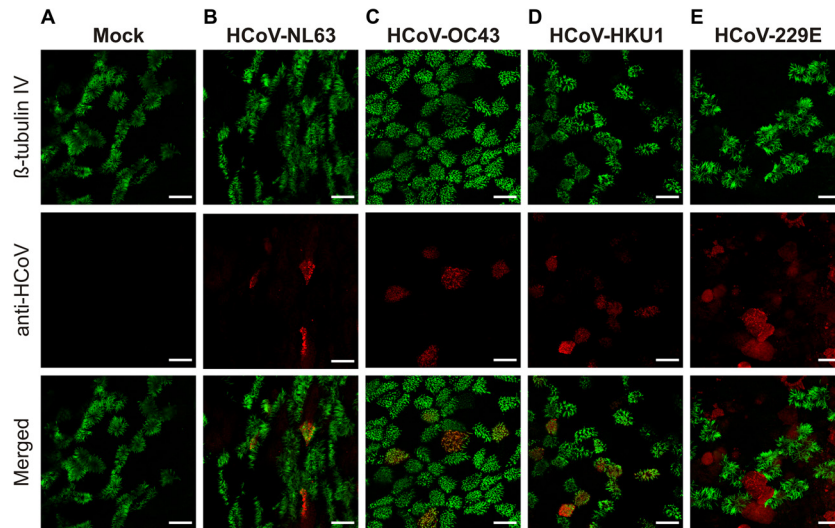


FIG 4 Cell tropisms of representative clinical HCoV isolates. Human airway epithelial cell cultures were fixed at 120 hpi, followed by double immunostaining with monoclonal anti- β -tubulin IV to detect ciliated cells (green) and human IVIg to detect HCoV proteins (red), and were then examined by confocal microscopy. Magnification, $\times 40$. Representative images at 120 hpi are presented for a control culture (A) and for HCoV-NL63 (B)-, HCoV-OC43 (C)-, HCoV-HKU1 (D)-, and HCoV-229E (E)-inoculated cultures. An overlay image was generated to determine the cell tropism of each HCoV isolate. Bars, 20 μm .

In addition, a tight junction marker (ZO-1) and a ciliated cell marker (β -tubulin) were incorporated to accurately discriminate the localization of the dsRNA complexes among different cell types present in the HAE cultures. The acquired z -stack images of both HAE cultures were processed and, as expected, demonstrated colocalization of dsRNA with the nonstructural viral protein (Fig. 5A). The inclusion of the cell-specific markers allowed a clear discrimination between nonciliated and ciliated cells and confirmed our previous finding that HCoV-229E infects predominantly nonciliated cells.

The dsRNA antibody staining in parallel with the cellular markers gave a more detailed view of the number of HCoV-infected cells. Therefore, we characterized the target cell tropisms of the different HCoV strains in HAE cultures quantitatively, using contemporary HCoV-229E (0349), HCoV-OC43 (0500), and HCoV-HKU1 (0315) isolates and the HCoV-NL63 (Ams-001)

reference strain. We inoculated HAE cultures from two donors with HCoVs and analyzed the samples at 48 and 96 hpi. For each HCoV strain, time point, and donor, we analyzed five randomly selected fields across the HAE culture, resulting in the analysis of more than 1,000 cells per virus strain. The cumulative immunostaining data show that a large number of replication complexes were detected at 48 and 96 hpi for HCoV-229E and HCoV-HKU1 for both donors (Table 2). In contrast, the numbers of dsRNA-positive cells for HCoV-NL63 and HCoV-OC43 were, on average, lower. These numbers corresponded with the RNA yields at the assessed time points for each of the viruses (Fig. 3). We used the cumulative data to calculate the colocalization percentages of dsRNA-positive cells with either ciliated or nonciliated cells (Fig. 5B). This quantitative analysis confirmed that HCoV-229E infects predominantly nonciliated cells ($P = 0.0030$), whereas HCoV-NL63 ($P = 0.0082$), HCoV-OC43 ($P = 0.0017$), and HCoV-

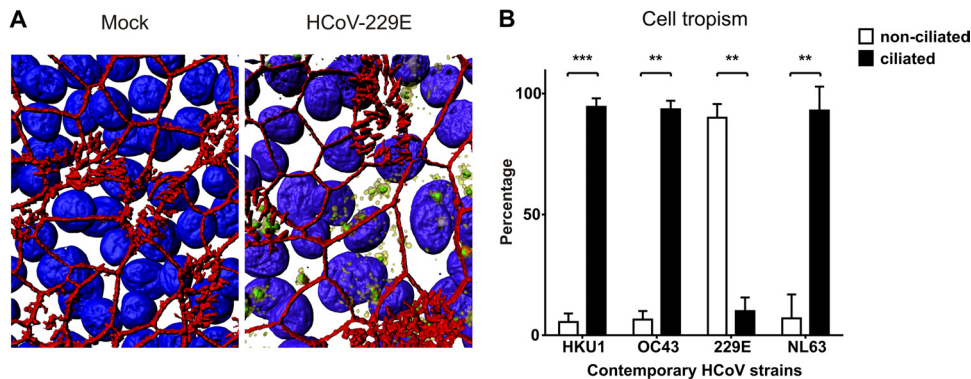


FIG 5 Quantification of human coronavirus cell tropism. (A) Representative transparent, three-dimensionally rendered z -stack images of HCoV-229E-infected and control HAE cell cultures are shown to illustrate the quantification method for HCoV cell tropism. The cultures were stained with antibodies directed against β -tubulin IV (ciliated cells; red), ZO1 (tight junctions; red), NSP8 (replication complexes; yellow), and dsRNA (viral dsRNA; green) and with DAPI (cell nucleus; blue). (B) Percentages of colocalization of dsRNA with nonciliated (white bars) and ciliated (black bars) cells of four contemporary HCoV strains at 96 hpi. The results are shown as means and SD for 5 randomly selected fields from 2 independent experiments. **, $P < 0.01$; ***, $P < 0.001$ (two-tailed, unpaired t test).

TABLE 2 Cumulative numbers of nonciliated and ciliated cells positive for dsRNA complexes

Donor	HCoV isolate	HCoV strain	Time point (hpi)	No. of cells		No. of cells positive for dsRNA	
				Nonciliated cells	Ciliated cells	Nonciliated cells	Ciliated cells
1212	349	229E	48	1,019	479	246	13
	349	229E	96	844	422	147	9
	Ams-001	NL63	48	960	530	8	20
	Ams-001	NL63	96	810	456	12	71
	315	HKU1	48	1,097	351	2	20
	315	HKU1	96	785	432	17	167
	500	OC43	48	908	379	0	0
	500	OC43	96	1,107	479	4	46
	Mock		48	1,120	447	0	0
	Mock		96	707	449	0	0
0712	349	229E	48	996	450	209	52
	349	229E	96	703	357	143	23
	Ams-001	NL63	48	960	494	0	21
	Ams-001	NL63	96	796	544	0	21
	315	HKU1	48	993	574	12	151
	315	HKU1	96	962	444	11	260
	500	OC43	48	965	552	1	11
	500	OC43	96	945	558	2	64
	Mock		48	1,100	557	0	0
	Mock		96	1,019	525	0	0

HKU1 ($P = 0.0007$) infect predominantly ciliated cells (Fig. 5B). Importantly, it also became apparent that the target cell tropism of each HCoV strain is not strictly limited to a certain cell type.

The target cell tropism of HCoV-NL63 correlates with the distribution pattern of its cellular receptor, angiotensin converting enzyme II, which is expressed predominantly on ciliated cells (39). HCoV-229E utilizes human aminopeptidase N (CD13) as a cellular receptor; however, the distribution pattern of this receptor on human airway epithelial cells has not been defined (40). Therefore, we assessed the distribution pattern of human aminopeptidase N (CD13) *in vivo* and *in vitro*, using bronchial lung resections and pseudostratified HAE cultures. This revealed that human aminopeptidase N colocalizes with nonciliated cells (Fig. 6), suggesting that, like that of HCoV-NL63, the HCoV-229E target cell tropism is determined by the receptor distribution in the human airway epithelium (52). We hypothesize that this is also the case for HCoV-OC43 and HCoV-HKU1; however, for both viruses, the functional cellular receptor is unknown.

DISCUSSION

We show here that HAE cell culture is a robust and universal HCoV culture system that facilitates the isolation and characterization of HCoVs. A total of 10 contemporary HCoV strains were obtained directly from clinical specimens. Analysis of the target cell tropisms of HCoV-HKU1, HCoV-229E, HCoV-OC43, and HCoV-NL63 at the primary entry port of infection revealed that HCoV-229E has a preference to infect nonciliated cells, whereas HCoV-NL63, HCoV-HKU1, and HCoV-OC43 all prefer ciliated cells.

Although HCoV-OC43 and HCoV-229E have been known since the mid-1960s (4, 5), their target cell tropisms on HAE cells were previously unknown. HCoV-OC43 infects predominantly ciliated cells, with apical release of progeny virus, similar to

HCoV-NL63 and HCoV-HKU1 (25, 41). Regarding HCoV-229E, Wang et al. previously showed that HCoV-229E can infect HAE cultures; however, in that study, no cell tropism of the virus or phenotype of the cells that expressed CD13 was defined (40). Therefore, the different cell tropism of HCoV-229E from that of the other three HCoV strains remained unknown.

The property of a virus to secrete progeny to the apical or basolateral surface, or bilaterally, may be decisive for subsequent virus spread and, possibly, disease outcome. Respiratory viruses that can cross the epithelial barrier have the opportunity to infect other types of cells that harbor the same cellular receptor. For several respiratory viruses, including HCoV-229E, HCoV-HKU1,

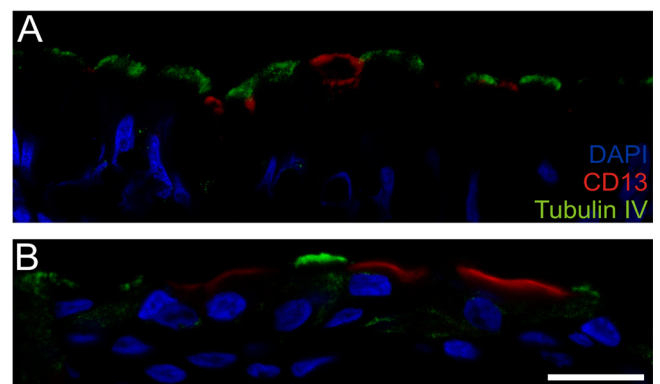


FIG 6 *In vivo* and *in vitro* distributions of CD13 expression in human airway epithelium. Human bronchial tissue segments (A) and pseudostratified HAE cultures (B) were stained with antibodies directed against β -tubulin IV (ciliated cells; green) and human CD13 (red) and with DAPI (cell nucleus; blue) to determine the receptor distribution. Confocal images representative of 5 randomly selected fields from 2 independent experiments are shown. Bar, 20 μ m.

and SARS-CoV (25, 40, 42), the ability to cross the epithelial border by basolateral release of the virus has been determined via HAE cultures (43, 44). In the current study, we support the documented polarity of HCoV-229E and HCoV-HKU1 progeny viruses (apical infection and apical release) and demonstrate the same polarity for HCoV-NL63 and HCoV-OC43. This was not documented before for either HCoV-NL63 (26, 41) or HCoV-OC43. Our results suggest that the apical-apical polarity of HCoVs restricts these viruses to the airway lumen. Interestingly, we did not detect any cytopathic effect in HAE cultures that had been infected with HCoVs, suggesting that apical release of progeny virus is the predominant viral exit route as long as the epithelium remains intact. We observed no visual changes in cell layer confluence, morphology, or cilium movement in HCoV-infected HAE cultures at 120 hpi. This was also reflected by the lack of disruption of the tight junction barriers, a marker for pseudostratified cell layer integrity. Furthermore, the cumulative data on the numbers of ciliated and nonciliated cells among the different HAE cultures also revealed no remarkable differences in the cell populations (Table 2). Therefore, HCoVs infect HAE cultures without inducing gross pathological changes. These results are in accordance with what has been reported previously for other respiratory viruses (24, 44, 45); however, we did not investigate transepithelial resistance, dead cell shedding, or if the cilium beating frequency was reduced during infection, as shown earlier for HCoV-229E in experimentally inoculated human volunteers (46). This physiological effect has been shown to be involved in the congestion and accumulation of mucus of the upper airways, which are hallmarks of the common cold (46). Future studies with HAE cultures should address whether the cilium beating frequency is altered upon HCoV infection alone or in combination with increased mucus secretion. It is also important that macrophages and dendritic cells (DCs) are likely to play a role during viral replication in the lung. This is particularly interesting because HCoV-229E is known to replicate efficiently in macrophages and DCs. Therefore, it will be important in future studies to complement HAE cultures with macrophages and DCs and to assess if basolateral release of progeny virus can be observed. HAE cocultures with macrophages and DCs will also be interesting in the context of host responses, such as release of proinflammatory cytokines that may confer cytopathogenicity and thus facilitate basolateral virus release.

The difficulty in acquiring new HCoV-NL63 isolates from clinical specimens suggests that this virus is more fastidious than the other HCoV strains. Only one novel HCoV-NL63 isolate was obtained, although six attempts were performed here. Indeed, the difficulty in culturing this strain was suspected in light of the late discovery of HCoV-NL63, in 2004, 40 years after HCoV-229E and HCoV-OC43 were discovered (19). Failure to culture HCoV-NL63 from clinical specimens, even those with high viral loads, suggests that other factors might be involved in successful HCoV-NL63 culture, e.g., neutralizing antibodies or inhibitory cytokines and/or chemokines in a specimen. However, we cannot exclude the possibility that factors affecting sample quality may have been involved in the observed difficulty in isolating HCoV-NL63 in our study. In contrast to HCoV-NL63, we readily obtained several HCoV-HKU1 isolates by using HAE cultures. Also, HCoV-HKU1 was discovered only recently (20), and in contrast to all other HCoV strains, propagation of HCoV-HKU1 is still not possible in any conventional cell line-based culture system. Therefore, it is

not surprising that HCoV-HKU1 was discovered only after intensified surveillance for coronaviruses in the human population following the SARS epidemic. Our finding that 4 of 12 HCoV-positive samples contained replication-competent HCoV-HKU1 confirms that HCoV-HKU1 is a contemporary HCoV strain and, furthermore, highlights the value of HAE cultures for the isolation of human respiratory viruses that are refractory to propagation in conventional cell lines.

Recombination is a major driving force of coronavirus evolution, and intraspecies recombination events have already been proposed for HCoV-OC43, -HKU1, and -NL63 (29, 47, 48). Among animal coronaviruses, type I and type II feline and canine coronaviruses are prominent examples of interspecies recombination (49). A prerequisite for recombination is coinfection of the same target cell, and our data suggest that there is a certain likelihood of HCoV-OC43, HCoV-HKU1, and HCoV-NL63 coinfection in the human airway epithelium. With the current knowledge on target cell tropism and the availability of a reverse genetic system for most HCoVs, it is now possible to address this question experimentally within the native environment (27, 41, 50).

Finally, the HAE culture system will also greatly facilitate assessments of the zoonotic potential of coronaviruses. The rapid expansion of the number of novel identified CoV species in various members of mammals and birds indicates that it is not unlikely that additional CoVs will be identified in the years to come (2). Notably, more than 50 newly identified CoVs have been detected in various bat species alone, including close relatives to SARS-CoV and HCoV-229E (2, 51). Thus, it has been proposed that bats are the reservoir of most, if not all, known CoVs (51). The emergence of SARS-CoV and the recently discovered novel human betacoronavirus HCoV-EMC, which both most likely originated from bat coronaviruses, shows that CoV cross-species transmission and adaptation to the human population can occur (17). Although these viruses are easily culturable on Vero cells, the HAE culture system allows detailed characterization of the cell tropism and apical/basolateral release of zoonotic CoVs. We expect that the HAE culture system will greatly facilitate the isolation of emerging respiratory virus strains that are refractory to growth on conventional cell lines and will help to address the question of whether such emerging viruses can replicate efficiently on the human airway epithelium. Most importantly, it will also allow the testing of potentially efficacious therapeutic options in a relevant *in vitro* cell culture model to combat emerging respiratory viruses.

ACKNOWLEDGMENTS

We gratefully thank Regulo Rodriguez for providing pathologically examined surgical lung resections and John Ziebuhr for providing the antiserum directed against HCoV-229E NSP8.

This study was supported by a Sixth Framework grant (LSHM-CT-2006-037276) from the European Union, a VIDU grant (016.066.318) from the Netherlands Organization for Scientific Research (NWO), the Sixth Framework Programme under the project GRACE (EC grant LSHM-CT-2005-518226), the Swiss National Science Foundation (project 31003A_132898), and the 3R Research Foundation Switzerland (project 128-11).

REFERENCES

1. Lai MMC, Perlman S, Anderson JL. 2007. Coronaviridae, p 1305–1335. In Knipe DM, Howley PM, Griffin DE, Lamb RA, Martin MA, Roizman B, Straus SE (ed), *Fields virology*, 5th ed. Lippincott Williams & Wilkins, Philadelphia, PA.

2. Perlman S, Netland J. 2009. Coronaviruses post-SARS: update on replication and pathogenesis. *Nat. Rev. Microbiol.* 7:439–450. doi:10.1038/nrmicro2147.
3. Weiss SR, Navas-Martin S. 2005. Coronavirus pathogenesis and the emerging pathogen severe acute respiratory syndrome coronavirus. *Microbiol. Mol. Biol. Rev.* 69:635–664.
4. Hamre D, Procknow JJ. 1966. A new virus isolated from the human respiratory tract. *Proc. Soc. Exp. Biol. Med.* 121:190–193.
5. McIntosh K, Dees JH, Becker WB, Kapikian AZ, Chanock RM. 1967. Recovery in tracheal organ cultures of novel viruses from patients with respiratory disease. *Proc. Natl. Acad. Sci. U. S. A.* 57:933–940.
6. Bradburne AF, Bynoe ML, Tyrrell DA. 1967. Effects of a “new” human respiratory virus in volunteers. *Br. Med. J.* 3:767–769.
7. Falsely AR, McCann RM, Hall WJ, Criddle MM, Formica MA, Wycoff D, Kolassa JE. 1997. The “common cold” in frail older persons: impact of rhinovirus and coronavirus in a senior daycare center. *J. Am. Geriatr. Soc.* 45:706–711.
8. Kraaijeveld CA, Reed SE, Macnaughton MR. 1980. Enzyme-linked immunosorbent assay for detection of antibody in volunteers experimentally infected with human coronavirus strain 229E. *J. Clin. Microbiol.* 12:493–497.
9. Macnaughton MR, Hasony HJ, Madge MH, Reed SE. 1981. Antibody to virus components in volunteers experimentally infected with human coronavirus 229E group viruses. *Infect. Immun.* 31:845–849.
10. Reed SE. 1984. The behaviour of recent isolates of human respiratory coronavirus in vitro and in volunteers: evidence of heterogeneity among 229E-related strains. *J. Med. Virol.* 13:179–192.
11. van der Hoek L. 2007. Human coronaviruses: what do they cause? *Antivir. Ther.* 12:651–658.
12. Drosten C, Gunther S, Preiser W, van der Werf S, Brodt HR, Becker S, Rabenau H, Panning M, Kolesnikova L, Fouchier RA, Berger A, Burguiera AM, Cinatl J, Eickmann M, Escriou N, Grywna K, Kramme S, Manuguerra JC, Muller S, Rickerts V, Sturmer M, Vieth S, Klenk HD, Osterhaus AD, Schmitz H, Doerr HW. 2003. Identification of a novel coronavirus in patients with severe acute respiratory syndrome. *N. Engl. J. Med.* 348:1967–1976. doi:10.1056/NEJMoa030747.
13. Fouchier RA, Kuiken T, Schutten M, van Amerongen G, van Doornum GJ, van den Hoogen BG, Peiris M, Lim W, Stohr K, Osterhaus AD. 2003. Aetiology: Koch’s postulates fulfilled for SARS virus. *Nature* 423:240. doi:10.1038/423240a.
14. Marra MA, Jones SJ, Astell CR, Holt RA, Brooks-Wilson A, Butterfield YS, Khattri J, Asano JK, Barber SA, Chan SY, Cloutier A, Coughlin SM, Freeman D, Girn N, Griffith OL, Leach SR, Mayo M, McDonald H, Montgomery SB, Pandoh PK, Petrescu AS, Robertson AG, Schein JE, Siddiqui A, Smailus DE, Stott JM, Yang GS, Plummer F, Andonov A, Artsob H, Bastien N, Bernard K, Booth TF, Bowness D, Czub M, Drebot M, Fernando L, Flick R, Garbutt M, Gray M, Grolla A, Jones S, Feldmann H, Meyers A, Kabani A, Li Y, Normand S, Stroher U, Tipples GA, Tyler S, Vogrig R, Ward D, Watson B, Brunham RC, Kraiden M, Petric M, Skowronski DM, Upton C, Roper RL. 2003. The genome sequence of the SARS-associated coronavirus. *Science* 300:1399–1404. doi:10.1126/science.1085953.
15. Perlman S, Dandekar AA. 2005. Immunopathogenesis of coronavirus infections: implications for SARS. *Nat. Rev. Immunol.* 5:917–927. doi:10.1038/nri1732.
16. Rota PA, Oberste MS, Monroe SS, Nix WA, Campagnoli R, Icenogle JP, Penaranda S, Bankamp B, Maher K, Chen MH, Tong S, Tamin A, Lowe L, Frace M, DeRisi JL, Chen Q, Wang D, Erdman DD, Peret TC, Burns C, Ksiazek TG, Rollin PE, Sanchez A, Liffick S, Holloway B, Limor J, McCaustland K, Olsen-Rasmussen M, Fouchier R, Gunther S, Osterhaus AD, Drosten C, Pallansch MA, Anderson LJ, Bellini WJ. 2003. Characterization of a novel coronavirus associated with severe acute respiratory syndrome. *Science* 300:1394–1399. doi:10.1126/science.1085952.
17. Zaki AM, van Boheemen S, Bestebroer TM, Osterhaus AD, Fouchier RA. 2012. Isolation of a novel coronavirus from a man with pneumonia in Saudi Arabia. *N. Engl. J. Med.* 367:1814–1820. doi:10.1056/NEJMoa1211721.
18. Fouchier RA, Hartwig NG, Bestebroer TM, Niemeyer B, de Jong JC, Simon JH, Osterhaus AD. 2004. A previously undescribed coronavirus associated with respiratory disease in humans. *Proc. Natl. Acad. Sci. U. S. A.* 101:6212–6216.
19. van der Hoek L, Pyrc K, Jebbink MF, Vermeulen-Oost W, Berkhout RJ, Wolthers KC, Wertheim-van Dillen PM, Kaandorp J, Spaargaren J, Berkhout B. 2004. Identification of a new human coronavirus. *Nat. Med.* 10:368–373. doi:10.1038/nm1024.
20. Woo PC, Lau SK, Chu CM, Chan KH, Tsoi HW, Huang Y, Wong BH, Poon RW, Cai JJ, Luk WK, Poon LL, Wong SS, Guan Y, Peiris JS, Yuen KY. 2005. Characterization and complete genome sequence of a novel coronavirus, coronavirus HKU1, from patients with pneumonia. *J. Virol.* 79:884–895.
21. Dijkman R, Jebbink MF, Gaunt E, Rossen JW, Templeton KE, Kuijpers TW, van der Hoek L. 2012. The dominance of human coronavirus OC43 and NL63 infections in infants. *J. Clin. Virol.* 53:135–139.
22. Tyrrell DA, Bynoe ML, Hoorn B. 1968. Cultivation of “difficult” viruses from patients with common colds. *Br. Med. J.* 1:606–610.
23. Tyrrell DAJ, Bynoe ML. 1965. Cultivation of novel type of common-cold virus in organ cultures. *Br. Med. J.* 1:1467–1470.
24. Dijkman R, Koekoek SM, Molenkamp R, Schildgen O, van der Hoek L. 2009. Human bocavirus can be cultured in differentiated human airway epithelial cells. *J. Virol.* 83:7739–7748.
25. Pyrc K, Sims AC, Dijkman R, Jebbink M, Long C, Deming D, Donaldson E, Vabret A, Baric R, van der Hoek L, Pickles R. 2010. Culturing the unculturable: human coronavirus HKU1 infects, replicates, and produces progeny virions in human ciliated airway epithelial cell cultures. *J. Virol.* 84:11255–11263.
26. Banach S, Orenstein JM, Fox LM, Randell SH, Rowley AH, Baker SC. 2009. Human airway epithelial cell culture to identify new respiratory viruses: coronavirus NL63 as a model. *J. Virol. Methods* 156:19–26.
27. Thiel V, Herold J, Schelle B, Siddell SG. 2001. Infectious RNA transcribed in vitro from a cDNA copy of the human coronavirus genome cloned in vaccinia virus. *J. Gen. Virol.* 82:1273–1281.
28. Jansen RR, Schinkel J, Koekoek S, Pajkrt D, Beld M, de Jong MD, Molenkamp R. 2011. Development and evaluation of a four-tube real-time multiplex PCR assay covering fourteen respiratory viruses, and comparison to its corresponding single target counterparts. *J. Clin. Virol.* 51:179–185.
29. Pyrc K, Dijkman R, Deng L, Jebbink MF, Ross HA, Berkhout B, van der Hoek L. 2006. Mosaic structure of human coronavirus NL63, one thousand years of evolution. *J. Mol. Biol.* 364:964–973.
30. Fulcher ML, Gabriel S, Burns KA, Yankaskas JR, Randell SH. 2005. Well-differentiated human airway epithelial cell cultures, p 183–206. *In* Picot J (ed), *Human cell culture protocols*, 2nd ed. Humana Press Inc, Totowa, NJ.
31. Boom R, Sol CJA, Salimans MMM, Jansen CL, Wertheim-van Dillen PME, Van der Noordaa J. 1990. A rapid and simple method for purification of nucleic acids. *J. Clin. Microbiol.* 28:495–503.
32. Schildgen O, Jebbink MF, de Vries M, Pyrc K, Dijkman R, Simon A, Muller A, Kupfer B, van der Hoek L. 2006. Identification of cell lines permissive for human coronavirus NL63. *J. Virol. Methods* 138:207–210.
33. Vijgen L, Keyaerts E, Moes E, Maes P, Duson G, Van RM. 2005. Development of one-step, real-time, quantitative reverse transcriptase PCR assays for absolute quantitation of human coronaviruses OC43 and 229E. *J. Clin. Microbiol.* 43:5452–5456.
34. Dijkman R, Jebbink MF, Deijs M, Milewska A, Pyrc K, Buelow E, van der Bijl A, van der Hoek L. 2012. Replication-dependent downregulation of cellular angiotensin-converting enzyme protein expression by human coronavirus NL63. *J. Gen. Virol.* 93:1924–1992. doi:10.1099/vir.0.043919-0.
35. Ziebuhr J, Siddell SG. 1999. Processing of the human coronavirus 229E replicase polyproteins by the virus-encoded 3C-like proteinase: identification of proteolytic products and cleavage sites common to pp1a and pp1ab. *J. Virol.* 73:177–185.
36. Dijkman R, Jebbink MF, Wilbrink B, Pyrc K, Zaaier HL, Minor PD, Franklin S, Berkhout B, Thiel V, van der Hoek L. 2006. Human coronavirus 229E encodes a single ORF4 protein between the spike and the envelope genes. *Virol. J.* 3:106. doi:10.1186/1743-422X-3-106.
37. Farsani SM, Dijkman R, Jebbink MF, Goossens H, Ieven M, Deijs M, Molenkamp R, van der Hoek L. 2012. The first complete genome sequences of clinical isolates of human coronavirus 229E. *Virus Genes* 45:433–439. doi:10.1007/s11262-012-0807-9.
38. Schonborn J, Oberstrass J, Breyel E, Tittgen J, Schumacher J, Lukacs N. 1991. Monoclonal antibodies to double-stranded RNA as probes of RNA structure in crude nucleic acid extracts. *Nucleic Acids Res.* 19:2993–3000.
39. Jia HP, Look DC, Shi L, Hickey M, Pewe L, Netland J, Farzan M, Wohlford-Lenane C, Perlman S, McCray PB, Jr. 2005. ACE2 receptor expression and severe acute respiratory syndrome coronavirus infection

- depend on differentiation of human airway epithelia. *J. Virol.* 79:14614–14621.
40. Wang G, Deering C, Macke M, Shao J, Burns R, Blau DM, Holmes KV, Davidson BL, Perlman S, McCray PB, Jr. 2000. Human coronavirus 229E infects polarized airway epithelia from the apical surface. *J. Virol.* 74:9234–9239.
 41. Donaldson EF, Yount B, Sims AC, Burkett S, Pickles RJ, Baric RS. 2008. Systematic assembly of a full-length infectious clone of human coronavirus NL63. *J. Virol.* 82:11948–11957.
 42. Sims AC, Baric RS, Yount B, Burkett SE, Collins PL, Pickles RJ. 2005. Severe acute respiratory syndrome coronavirus infection of human ciliated airway epithelia: role of ciliated cells in viral spread in the conducting airways of the lungs. *J. Virol.* 79:15511–15524.
 43. Rowe RK, Pekosz A. 2006. Bidirectional virus secretion and nonciliated cell tropism following Andes virus infection of primary airway epithelial cell cultures. *J. Virol.* 80:1087–1097.
 44. Zhang L, Peeples ME, Boucher RC, Collins PL, Pickles RJ. 2002. Respiratory syncytial virus infection of human airway epithelial cells is polarized, specific to ciliated cells, and without obvious cytopathology. *J. Virol.* 76:5654–5666.
 45. Zhang L, Bukreyev A, Thompson CI, Watson B, Peeples ME, Collins PL, Pickles RJ. 2005. Infection of ciliated cells by human parainfluenza virus type 3 in an in vitro model of human airway epithelium. *J. Virol.* 79:1113–1124.
 46. Chilvers MA, McKean M, Rutman A, Myint BS, Silverman M, O'Callaghan C. 2001. The effects of coronavirus on human nasal ciliated respiratory epithelium. *Eur. Respir. J.* 18:965–970.
 47. Lau SK, Lee P, Tsang AK, Yip CC, Tse H, Lee RA, So LY, Lau YL, Chan KH, Woo PC, Yuen KY. 2011. Molecular epidemiology of human coronavirus OC43 reveals evolution of different genotypes over time and recent emergence of a novel genotype due to natural recombination. *J. Virol.* 85:11325–11337.
 48. Woo PC, Lau SK, Yip CC, Huang Y, Tsoi HW, Chan KH, Yuen KY. 2006. Comparative analysis of 22 coronavirus HKU1 genomes reveals a novel genotype and evidence of natural recombination in coronavirus HKU1. *J. Virol.* 80:7136–7145.
 49. Herrewegh AA, Smeenk I, Horzinek MC, Rottier PJ, de Groot RJ. 1998. Feline coronavirus type II strains 79-1683 and 79-1146 originate from a double recombination between feline coronavirus type I and canine coronavirus. *J. Virol.* 72:4508–4514.
 50. St-Jean JR, Desforgues M, Almazan F, Jacomy H, Enjuanes L, Talbot PJ. 2006. Recovery of a neurovirulent human coronavirus OC43 from an infectious cDNA clone. *J. Virol.* 80:3670–3674.
 51. Pfefferle S, Oppong S, Drexler JF, Gloza-Rausch F, Ipsen A, Seebens A, Muller MA, Annan A, Vallo P, Adu-Sarkodie Y, Kruppa TF, Drosten C. 2009. Distant relatives of severe acute respiratory syndrome coronavirus and close relatives of human coronavirus 229E in bats, Ghana. *Emerg. Infect. Dis.* 15:1377–1384.
 52. Bertram S, Dijkman R, Habjan M, Heurich A, Gierer S, Glowacka I, Welsch K, Winkler M, Schneider H, Hofmann-Winkler H, Thiel V, Pöhlmann S. 2013. TMPRSS2 activates the human coronavirus 229E for cathepsin-independent host cell entry and is expressed in viral target cells in the respiratory epithelium. *J. Virol.* 87:6150–6160.